Inversion electrons on narrow-band-gap semiconductors in crossed electric and magnetic fields

W. Zawadzki,* S. Klahn, and U. Merkt
Institut für Angewandte Physik, Universität Hamburg, D-2000 Hamburg 36, Federal Republic of Germany
(Received 9 December 1985)

Electrons in inversion layers of narrow-band-gap semiconductors in the presence of an external magnetic field parallel to the interface (crossed-field configuration) are considered theoretically. A three-level model of the $\kappa \cdot \mathbf{P}$ theory is used to describe electrons in external electric and magnetic fields, taking into account the main features of the band structure in InSb-type semiconductors: a small energy gap and a strong spin-orbit interaction. The electric potential is taken to be in the form of a triangular well and the presence of the interface is accounted for by appropriate boundary conditions for the wave function. An analytic description of the eigenenergies is obtained for arbitrary intensities of the homogeneous electric and magnetic fields, from magnetic surface levels (vanishing electric field) to purely electric subbands (vanishing magnetic field). Experimental data on electron cyclotron resonance in InSb in the presence of crossed fields (the bulk limit) are theoretically described and interpreted using an analogy between electrons in narrow-gap semiconductors and relativistic electrons in vacuum. The influence of a transverse magnetic field on the energies of intersubband resonances in metal-oxide-semiconductor structures is discussed. The relation of the theoretical results obtained to existing and possible experiments is emphasized throughout.

I. INTRODUCTION

Investigations of electrons in semiconductors in the presence of crossed magnetic and electric fields offer interesting physical possibilities, both experimental and theoretical.[1] The crossed-field configuration is fundamental for classical and quantum transport phenomena in solids and it has attracted a renewed interest in connection with the discovery of the quantum-Hall effect in two-dimensional systems.[2] It has been predicted that in narrow-band-gap semiconductors the crossed-field case could serve as an example of a "semirelativistic" electron behavior, governed by the energy-momentum relation analogous to that for free electrons in vacuum.[3]

Optical investigations of bulk semiconductors in crossed magnetic and electric fields began with a theoretical work of Hensel and Peter,[4] who indicated that an influence of electric field on Landau levels should lead to observable effects in cyclotron resonance transitions in degenerate valence bands of Γ_8 symmetry, and with the work of Aronov,[5] who pointed out that electric field effects should be visible in interband magneto-optical transitions. This was followed by the pioneering experimental work of Vrehen *et al.*,[6] who used germanium *p-n* junctions in order to apply electric fields up to 5×10^4 V/cm in interband magneto-optical investigations. It was observed that at low E/B values, one deals with magnetic-type electron and hole behavior, leading to oscillatory magnetoabsorption and dispersion effects, whereas at large E/B ratios, one deals with nonquantized electric-type behavior, leading to nonoscillatory Franz-Keldysh effect. This behavior was not understood in the framework of one-band effective-mass approximation (EMA), which predicted magnetic-type behavior for all E/B ratios, as long as electron scattering was negligible. The puzzle was resolved by Zak and Zawadzki,[7] who showed that the validity itself of the one-band EMA implies that the E/B ratio is not too large. Then the two-band EMA description for crossed fields was developed, which correctly predicted both types of behavior.[8–10] New intraband magneto-optical transitions in crossed fields were described for nonparabolic bands of narrow-band-gap semiconductors.[11]

However, the experimental work performed with the use of crossed fields has, until present, been limited to germanium, which is not a narrow-band-gap semiconductor, and to interband experiments, whose interpretation has been obscured by the degenerate character of the valence band in this material. Only recently has it become possible to apply high electric fields to narrow-gap semiconductors, owing to advanced technology of metal-oxide-semiconductor (MOS) structures.[12] The surface electric field in a MOS structure (as well as in a semiconductor heterojunction) is transverse to the interface, so that directing an external magnetic field parallel to the interface one creates a crossed-field configuration for the inversion charge carriers. An important feature, which considerably simplifies interpretation of intraband optical experiments is an absence of the plasma shift in such a structure.[13,14]

When working with MOS or heterojunction structures one must take into account the presence of an interface. This aspect of the problem is related to investigations of magnetic surface levels in metals and semimetals, in which one studies electron orbits near the metal surface in the presence of a magnetic field. As the electromagnetic radiation may not penetrate the metal bulk, one is able to observe exclusively the surface states within the skin-depth layer near the surface. Since in metals and semimetals the Fermi energy is high in the band and many Landau levels are populated, one deals with high quantum numbers and the semiclassical quantization pro-

cedure is applicable.[15,16]

The spacing of levels due to magnetic quantization is proportional to $1/m^*$, while the spacing due to quantization in a constant electric field (triangular potential) is proportional to $(1/m^*)^{1/3}$. Hence, in semiconductors with large effective masses (like Si or GaAs), one may treat the effect of a magnetic field parallel to the interface as small and use a perturbation procedure for its description.[17,18] However, in narrow-gap semiconductors with small effective masses of charge carriers, the magnetic and electric effects are comparable in magnitude, the perturbation procedure is not applicable, and one must find a description of electron motion in the presence of crossed fields and a barrier treating both fields on an equal basis. This is the purpose of the present paper.

Since we are interested in narrow-gap semiconductors of InSb type, the description must take into account the real band structure of these materials, i.e., a small energy gap (leading to a strong interband $\mathbf{k}\cdot\mathbf{p}$ coupling and resulting in the band's nonparabolicity) and a strong spin-orbit interaction (resulting in a large spin-splitting Landé factor). The simplest description accounting for these features is provided by a three-level model of band structure, which we use throughout. The model also has the important property of describing both magnetic type and electric type of motion, depending on relative intensities of the two fields. However, as will be seen from the following considerations, the presence of a barrier tends to make the electron motion more "electric," so that the distinction between both types of behavior is not as dramatic as in the purely three-dimensional case. The main simplification of our description is related to a triangular electric potential, i.e., to the assumption that an electric field confining electrons in an inversion layer is constant in space. We do not attempt self-consistent calculations of the potential, which, for the realistic band structure and in the presence of an external magnetic field, would represent a formidable numerical problem. As shown below, for homogeneous electric and magnetic fields perpendicular to each other we can obtain analytical eigenenergies for arbitrary field intensities from the magnetic surface states ($B\neq 0$, $E=0$) to the purely electric subbands ($B=0$, $E\neq 0$). The simplicity of the results allows us a clear physical interpretation.

In the second section we present the $\boldsymbol{\kappa}\cdot\mathbf{P}$ theory for electrons in magnetic and electric fields and specify the three-level model of band structure. In the third section, the eigenenergies for the magnetic type of motion are obtained and a bulk limit of the magnetic case is considered. Magnetic surface states are described ($E=0$ case). Further, the electric type of motion is treated and the eigenenergies are obtained using semiclassical quantization. This section contains also description of electric subbands ($B=0$) in narrow-gap semiconductors. In Sec. IV we discuss the preceding results using mostly the above-mentioned analogy between electrons in narrow-gap semiconductors and relativistic electrons in vacuum. Section V contains a brief summary.

II. $\boldsymbol{\kappa}\cdot\mathbf{P}$ THEORY

A. General theory

In this section we describe the $\mathbf{k}\cdot\mathbf{p}$ theory for conduction electrons in small-gap semiconductors in the presence of crossed electric and magnetic fields.

The initial Hamiltonian for our problem reads

$$H=\frac{1}{2m_0}P^2+U(\mathbf{r})+V_0(\mathbf{r}) +\frac{\hbar}{4m_0^2c^2}(\sigma\times\nabla V_0)\cdot\mathbf{P}+\mu_B\mathbf{B}\cdot\sigma\ , \tag{1}$$

where $\mathbf{P}=\mathbf{p}+e\mathbf{A}$ is the kinetic momentum. $\mathbf{A}$ is the vector potential of the magnetic field $\mathbf{B}$, e is the absolute value of the electron charge, m_0 is the free electron mass, μ_B is the Bohr magneton, and σ are the Pauli spin operators. $V_0(\mathbf{r})$ denotes the periodic potential energy of the lattice and $U(\mathbf{r})$ is the slowly varying electric potential energy due to external electric field. The spin-orbit interaction and the Pauli term are written in the standard form. We shall present here a derivation of the $\boldsymbol{\kappa}\cdot\mathbf{P}$ theory without going to the k space. The derivation is valid as long as the vector and the scalar potentials are slowly varying functions over a unit cell.

We look for the solution of the eigenvalue problem

$$H\Psi=\varepsilon\Psi \tag{2}$$

in the form

$$\Psi(\mathbf{r})=\sum_l f_l(\mathbf{r})u_l(\mathbf{r})\ , \tag{3}$$

where the summation is over the energy bands. $u_l(r)$ are the periodic parts of Bloch functions taken at $k=0$ (the Luttinger-Kohn-amplitudes), satisfying the eigenvalue problem

$$\left[\frac{1}{2m_0}P^2+V_0(\mathbf{r})+\frac{\hbar}{4m_0^2c^2}(\sigma\times\nabla V_0)\cdot\mathbf{p}\right]u_l(\mathbf{r})=\varepsilon_l u_l(\mathbf{r})\ . \tag{4}$$

ε_l denote the band-edge energies at the point Γ. Functions $u_l(\mathbf{r})$ are orthonormal: $(1/\Omega)\langle u_l\,|\,u_{l'}\rangle=\delta_{ll'}$ where the integral is carried over the volume of the unit cell Ω. On the other hand, the envelope functions $f_l(\mathbf{r})$ are slowly varying over the unit cell. Inserting Eq. (3) into Eqs. (2) and (1), we obtain

$$\sum_l\left[\frac{1}{2m_0}(p^2u_l)+\frac{1}{m_0}(\mathbf{p}u_l)\cdot\mathbf{p}+\frac{1}{2m_0}u_lp^2+\frac{e}{2m_0}(\mathbf{p}u_l)\cdot\mathbf{A}+\frac{e}{2m_0}u_l(\mathbf{p}\cdot\mathbf{A})+\frac{e}{2m_0}\mathbf{A}\cdot(\mathbf{p}u_l)+\frac{e}{2m_0}u_l(\mathbf{A}\cdot\mathbf{p}) +\frac{e^2}{2m_0}u_lA^2+Uu_l+V_0u_l+\frac{\hbar}{4m_0^2c^2}(\sigma\times\nabla V_0)\cdot(\mathbf{p}u_l)+\frac{\hbar}{4m_0^2c^2}u_l(\sigma\times\nabla V_0)\cdot\mathbf{p} +\frac{\hbar}{4m_0^2c^2}u_l(\sigma\times\nabla V_0)\cdot e\mathbf{A}+\mu_B\mathbf{B}\cdot\sigma u_l\right]f_l(\mathbf{r})=\varepsilon\sum_l f_l(\mathbf{r})u_l\ . \tag{5}$$

In Eq. (5) we have neglected ∇U compared to much larger ∇V_0. We multiply both sides of Eq. (5) from the left by $(1/\Omega)u_l^*$, and integrate over the unit cell. Since $\mathbf{A}(\mathbf{r})$, $U(\mathbf{r})$, and $f_l(\mathbf{r})$ are slowly varying, they may be taken out of the integral sign. Making use of Eq. (4) and of the orthonormality of u_l, the initial eigenvalue problem takes the form

$$\sum_l \left[\left(\frac{1}{2m_0} P^2 + \varepsilon_l + U - \varepsilon \right) \delta_{l'l} + \boldsymbol{\kappa}_{l'l} \cdot \mathbf{P} + \mu_B \mathbf{B} \cdot \boldsymbol{\sigma}_{l'l} \right] f_l(\mathbf{r}) = 0 , \tag{6}$$

where

$$\boldsymbol{\kappa}_{l'l} = \frac{1}{m_0} \langle u_{l'} \mid \mathbf{p} + \frac{\hbar}{4m_0 c^2} (\boldsymbol{\sigma} \times \nabla V_0) \mid u_l \rangle . \tag{7}$$

The above set of coupled differential equations for the envelope functions essentially contains no approximations. If the electric potential is due to a constant electric field, $U(r) = e\mathbf{E}\mathbf{r}$, then it is rigorously diagonal in the band index, even if it is not slowly varying over the unit cell.[7] The Pauli spin term in Eq. (6) contains both diagonal and nondiagonal terms.

In the procedure of Luttinger and Kohn,[19] one applies a canonical transformation in order to eliminate the off-diagonal part $\boldsymbol{\kappa}_{l'l} \cdot \mathbf{P}$ and to arrive at a one-band equation with an effective mass m_0^* replacing the free-electron mass m_0. This procedure is valid under certain restrictions, which depend on the problem in question (Zak and Zawadzki[7]). These restrictions may be generally summarized by the criterion that the electron energy counted from the bottom of the band must be small compared to the energy gap between the band in question and any other energy band. However, in small-gap semiconductors one often deals with electron or hole energies which are comparable to that of the gap. In such situations, the one-band equation is not applicable. The second approach, due to Kane,[20] essentially follows the procedure of perturbation theory for nearly degenerate levels: one considers a finite number of close-lying levels, treating them exactly and leaving out all other levels in the first approximation. We follow this scheme in our considerations of InSb-like semiconductors.

B. Three-level model

We consider a three-level model of the band structure at $k=0$ (the Γ point). The Γ_6 level (s type symmetry) is separated by the energy gap ε_g from the two-fold degenerate Γ_8 level (p type), which is in turn split off by the spin-orbit interaction Δ from the Γ_7 level (p type). In the following, we neglect the small spin-orbit contribution both in the interband matrix element of Eq. (7) and in Eq. (6). We also omit the free-electron term in the diagonal part and the Pauli spin term in Eq. (6), as they give only small contributions to the effective mass and the spin g value of electrons in InSb.

We choose, for the periodic parts of the Luttinger-Kohn functions, the following states (in the x,y,z crystal coordinate system), which diagonalize the Hamiltonian including the spin-orbit interaction to the first order of perturbation theory. The zero of energy is at the conduction-band edge:

$$\begin{aligned}
&u_1 = iS\uparrow, \quad \varepsilon_1 = 0 ; \\
&u_2 = iS\downarrow, \quad \varepsilon_2 = 0 ; \\
&u_3 = R_+\uparrow, \quad \varepsilon_3 = -\varepsilon_g ; \\
&u_4 = R_-\downarrow, \quad \varepsilon_4 = -\varepsilon_g ; \\
&u_5 = (\tfrac{1}{3})^{1/2} R_-\uparrow + (\tfrac{2}{3})^{1/2} Z\downarrow, \quad \varepsilon_5 = -\varepsilon_g ; \\
&u_6 = -(\tfrac{1}{3})^{1/2} R_+\downarrow + (\tfrac{2}{3})^{1/2} Z\uparrow, \quad \varepsilon_6 = -\varepsilon_g ; \\
&u_7 = -(\tfrac{2}{3})^{1/2} R_-\uparrow + (\tfrac{1}{3})^{1/2} Z\uparrow, \quad \varepsilon_7 = -\varepsilon_g - \Delta ; \\
&u_8 = (\tfrac{2}{3})^{1/2} R_+\downarrow + (\tfrac{1}{3})^{1/2} Z\downarrow, \quad \varepsilon_8 = -\varepsilon_g - \Delta ;
\end{aligned} \tag{8}$$

where $R_\pm = (X \pm iY)/\sqrt{2}$ and the symbols $\uparrow$ and $\downarrow$ denote spin-up and spin-down functions, respectively. S and X,Y,Z are periodic functions, which transform like atomic s and p functions under the operations of the tetrahedral group at the point Γ. Although we have neglected the spin-orbit contribution to the nondiagonal terms in the Hamiltonian, the zero-order functions do include the effect of the spin-orbit interaction. Making use of the identity

$$\boldsymbol{\kappa} \cdot \mathbf{P} = \kappa_+ P_- + \kappa_- P_+ + \kappa_z P_z ,$$

where $\kappa_\pm = (\kappa_x \pm i\kappa_y)/\sqrt{2}$ and $P_\pm = (P_x \pm iP_y)/\sqrt{2}$, the set of equations given in Eq. (6) can be represented (including the above-mentioned approximations) in the matrix form on the facing page [Eq. (9)], where $\kappa = -(i/m_0)\langle S \mid p_z \mid Z \rangle$.

In the following, we consider electrons in crossed magnetic and electric fields $\mathbf{B}=(0,0,B)$ and $\mathbf{E}=(0,E,0)$. We choose

$$\mathbf{A} = (-By,0,0), \quad U(\mathbf{r}) = eEy . \tag{10}$$

One can now express the envelope functions f_3, f_5, f_7 and f_4, f_6, f_8 by the functions f_1 and f_2, respectively, and substitute them into the first and fifth equation of the set given in Eq. (9). In doing this, one deals with terms proportional to commutators (P_y, eEy) (see, e.g., Ref. 21). These terms are responsible for Zener interband tunneling in the electric field,[22] but they give negligible contributions to electron energies as long as the energy gap ε_g is not too small.[23] Similar terms couple also f_1 and f_2 functions but, again, the coupling is very weak under usual experimental conditions.[24] Hence, in the following we neglect these terms. Taking into account the commutation rules

$$(P_x, P_y) = -ih^2/L^2, \quad (P_z, P_x) = (P_z, P_y) = 0 , \tag{11}$$

where $L = (\hbar/eB)^{1/2}$ is the Landau radius, we finally obtain the following decoupled equations for $f = f_1$ or $f = f_2$,

$$\left[(\varepsilon - U)(\varepsilon_g + \varepsilon - U)(\varepsilon_g + \Delta + \varepsilon - U) - (\varepsilon_g + \tfrac{2}{3}\Delta + \varepsilon - U)\kappa^2 P^2 \pm \tfrac{1}{3}\kappa^2 \frac{\hbar^2 \Delta}{L^2} \right] f(\mathbf{r}) = 0 , \tag{12}$$

$$
\begin{array}{c|cccccccc|c|c}
 & \kappa P_+ & \sqrt{1/3}\kappa P_- & -\sqrt{2/3}\kappa P_- & 0 & 0 & \sqrt{2/3}\kappa P_z & \sqrt{1/3}\kappa P_z & & \\
U-\varepsilon & -\varepsilon_g+U-\varepsilon & 0 & 0 & 0 & 0 & 0 & 0 & f_1 & \\
\kappa P_- & 0 & -\varepsilon_g+U-\varepsilon & 0 & 0 & 0 & 0 & 0 & f_3 & \\
\sqrt{1/3}\kappa P_+ & 0 & 0 & -\varepsilon_g-\Delta+U-\varepsilon & \sqrt{2/3}\kappa P_z & \sqrt{1/3}\kappa P_z & 0 & 0 & f_5 & \\
-\sqrt{2/3}\kappa P_+ & 0 & 0 & 0 & U-\varepsilon & \kappa P_- & -\sqrt{1/3}\kappa P_+ & \sqrt{2/3}\kappa P_+ & f_7 & =0 \\
0 & 0 & \sqrt{2/3}\kappa P_z & \sqrt{1/3}\kappa P_z & \kappa P_+ & -\varepsilon_g+U-\varepsilon & 0 & 0 & f_2 & \\
0 & 0 & 0 & 0 & -\sqrt{1/3}\kappa P_- & 0 & -\varepsilon_g+U-\varepsilon & 0 & f_4 & \\
\sqrt{2/3}\kappa P_z & 0 & 0 & 0 & \sqrt{2/3}\kappa P_- & 0 & 0 & -\varepsilon_g-\Delta+U-\varepsilon & f_6 & \\
\sqrt{1/3}\kappa P_z & 0 & 0 & 0 & 0 & 0 & 0 & 0 & f_8 &
\end{array}
\tag{9}
$$

where + and − signs correspond to f_1 and f_2 functions, respectively.

In the absence of external fields ($U=0$, $B=0$, $\mathbf{P}\rightarrow\hbar\mathbf{k}$), Eq. (12) reduces to the Kane dispersion relation for narrow-gap semiconductors.[20] In case of an external magnetic field, Eq. (12) reduces to the description of Landau levels obtained by Bowers and Yafet.[25] The last term within the large parentheses determines the spin splitting of levels due to magnetic field.

Equation (12) describes the conduction Γ_6 band, the light hole Γ_8 band, and the splitoff Γ_7 hole band. The heavy holes in the above three-level model are infinitely heavy ($\varepsilon=-\varepsilon_g$), since their finite mass results from $\mathbf{k}\cdot\mathbf{p}$ interaction with distant bands, not included in the above description.[20]

In order to make the solution of Eq. (12) more tractable, we consider the range of electron energies $\varepsilon\ll\varepsilon_g+2\Delta/3$. As it will be seen below, the strong inequality is not always valid for electrons in inversion layers on InSb ($\varepsilon_g+2\Delta/3=0.8$ eV). However, the above approximation furnishes a reasonable description, taking into account two essential features of the band structure: the nonparabolicity of the conduction band (due to the proximity of the valence band) and the large spin Landé factor (due to the strong spin-orbit interaction). For the above range of energies we may neglect $\varepsilon-U$ in comparison with $\varepsilon_g+2\Delta/3$ and $\varepsilon_g+\Delta$ in Eq. (12). Then we arrive at an equation that is quadratic in the energy ε and in the external electric potential. In view of the gauge chosen in Eq. (10) we may also separate the variables looking for solutions in the form

$$f_l(\mathbf{r})=\exp(ik_x x+ik_z z)\phi_l(y)\ . \tag{13}$$

After some manipulation, we obtain the following eigenvalue equations for the two projections of the total angular momentum $j=\pm\frac{1}{2}$:

$$\left[-\frac{\hbar^2}{2m_0^*}\frac{d^2}{dy^2}+\frac{m_0^*}{2}\omega^2(y-y_0)^2\right]\phi_\pm(y)=\beta_\pm\phi_\pm(y)\ , \tag{14}$$

where

$$\omega^2=\left[\frac{eB}{m_0^*}\right]^2-\frac{2e^2E^2}{m_0^*\varepsilon_g}\ , \tag{15}$$

$$y_0=-\frac{\alpha}{m_0^*\omega^2}\ , \tag{16}$$

$$\alpha=-\hbar k_x\frac{eB}{m_0^*}+eE\left[1+2\frac{\varepsilon}{\varepsilon_g}\right]\ , \tag{17}$$

$$\beta_\pm=\lambda_\pm+\frac{\alpha^2}{2m_0^*\omega^2}\ , \tag{18}$$

$$\lambda_\pm=\varepsilon\left[1+\frac{\varepsilon}{\varepsilon_g}\right]-\frac{\hbar^2k_x^2}{2m_0^*}-\frac{\hbar^2k_z^2}{2m_0^*}\pm\tfrac{1}{2}g_0^*\mu_B B\ . \tag{19}$$

The effective mass m_0^* and the Landé g factor at the band edge g_0^* are defined as

$$\frac{1}{m_0^*}=\frac{2\kappa^2}{3\varepsilon_g}\frac{2\Delta+3\varepsilon_g}{\Delta+\varepsilon_g}\ , \tag{20}$$

$$g_0^* = -\frac{m_0}{m_0^*}\frac{2\Delta}{2\Delta+3\varepsilon_g} . \tag{21}$$

In the following, we often use the cyclotron frequency $\omega_c = eB/m_0^*$ defined with the band-edge mass m_0^*.

Equation (14) looks similar to the eigenvalue equation for the harmonic oscillator centered at y_0. However, the boundary conditions for our problem are not those of the usual harmonic oscillator. Namely, we assume that the (x,z) plane at $y=0$ represents an interface between the semiconductor to the right and, e.g., an insulator to the left. The electron may not penetrate into the insulator, so that the wave functions should vanish at $y=0$ for an infinite potential barrier. In principle, as has been pointed out previously,[26] this boundary condition applies to the complete wave function Ψ, given in Eq. (3). However, in order to simplify the problem mathematically, we will approximate this condition assuming that, for the conduction band, it applies also to the main component of the wave function, i.e., to f_1 and to f_2 for the two spin orientations, respectively. Thus we impose the following approximate boundary conditions on the solutions of Eq. (14):

$$\phi_\pm(y)=0 \quad \text{for } y=0 \text{ and } y=+\infty . \tag{22}$$

The problem of correct boundary conditions is related to lifting of spin degeneracy due to an inversion asymmetry of the interface potential and the spin-orbit interaction.[26] However, since we are concerned with relatively strong magnetic fields, which result in large spin splittings of electron energies, we do not engage in inversion asymmetry considerations.

It follows from the form of Eq. (14) that we basically deal with two types of solutions, depending on the relative strengths of the magnetic and electric fields. The first type for $(eB/m_0^*)^2 > 2e^2E^2/m_0^*\varepsilon_g$ and the second type for $(eB/m_0^*)^2 < 2e^2E^2/m_0^*\varepsilon_g$. We tentatively call them the magnetic case and the electric case, respectively. However, as we show below, the presence of an interface [expressed by the boundary conditions in Eq. (22)] somewhat complicates this simple division.

III. ELECTRONS IN CROSSED FIELDS

In the next sections we present quantitative results for the eigenenergies of Eq. (14) with the boundary conditions of Eq. (22) and discuss their physical meaning.

A. Magnetic case: General

We consider first the magnetic case

$$\omega^2 = \omega_c^2(1-\gamma^2) > 0 , \tag{23}$$

where

$$\gamma^2 = \left[\frac{2m_0^*}{\varepsilon_g}\right]\left[\frac{E}{B}\right]^2 \tag{24}$$

is an important parameter for the problem. In the magnetic case there is $\gamma^2 < 1$ and, as follows from Eq. (15), we deal with electrons in a parabolic potential well centered at y_0. The influence of the barrier then depends strongly on the value of the center coordinate y_0, which determines the electron position with respect to the barrier, and on the value of ω, which determines the width of the well, i.e., the extent of the wave function. The corresponding classical electron trajectories are shown in Fig. 1. It is clear that the electron energies will depend strongly on y_0, if the electron is close enough to the barrier. If we divide Eq. (14) by $\hbar\omega$ and introduce the length

$$R = \left[\frac{\hbar}{2m_0^*\omega}\right]^{1/2} = \frac{L}{\sqrt{2}}(1-\gamma^2)^{-1/4} , \tag{25}$$

Eq. (14) takes the form

$$\left[\frac{d^2}{dq^2} - \tfrac{1}{4}(q-q_0)^2 - a\right]\phi(q)=0 , \tag{26}$$

where $q = y/R$, $q_0 = y_0/R$, and

$$a = -\frac{1}{\hbar\omega}\left[\lambda_\pm + \frac{\alpha^2}{2m_0^*\omega^2}\right] . \tag{27}$$

Equation (26) represents the standard form of the differential equation for the parabolic cylinder function.[27] The boundary conditions now read

$$\phi(q)=0 \quad \text{for } q=0 \text{ and } q=+\infty . \tag{28}$$

The electron energies can be obtained from Eq. (27) if the eigenvalues a of Eq. (26) are known. The latter can be

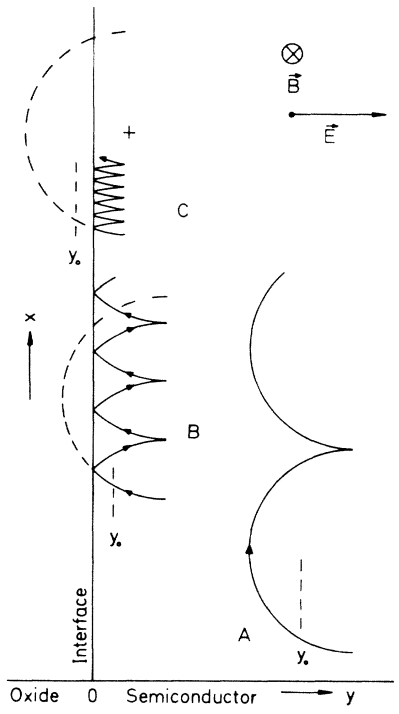

FIG. 1. Classical orbits of inversion electrons in a metal-oxide-semiconductor structure in the presence of crossed electric and magnetic fields $\mathbf{E}\perp\mathbf{B}$ for different electron positions y_0 (schematically). Orbit A lies inside the semiconductor and is not affected by the presence of the interface at $y=0$; orbits B and C result from periodic reflection at the interface.

given analytically to a good approximation for three ranges of q_0 values;

$$a_n \simeq \begin{cases} -(n+\frac{1}{2}) - \dfrac{1}{\sqrt{2\pi}} q_0^{2n+1} e^{-q_0^2/2} \dfrac{1}{n!}, & q_0 \gg 1 \quad (29a) \\ -(2n+\frac{3}{2}) + \dfrac{\sqrt{2}}{\pi} \dfrac{\Gamma(n+\frac{1}{2})}{n!} (2n+1) q_0, & |q_0| \lesssim 1 \quad (29b) \\ -\frac{1}{4} q_0^2 - [\frac{3}{4}\pi(n+\frac{3}{4}) q_0]^{2/3}, & q_0 \ll -1 \, . \quad (29c) \end{cases}$$

Equation (29a) has been derived by considering the asymptotic form of the parabolic cylinder functions for large negative arguments and looking for its zeros (for $q_0 \gg 1$ the argument $q - q_0$ at $q=0$ is large negative). In this case, the influence of the barrier is exponentially small, since the barrier occurs far away from the average electron position q_0, where the wave function already decays exponentially.

As far as the range of Eq. (29b) is concerned, the eigenvalues of Eq. (26) for $q_0=0$ are well known: $a_n(q_0=0) = -(2n+\frac{3}{2})$ for $n=0, 1, 2, \ldots$. They are obtained observing that in this particular case Eqs. (26) and (28) are satisfied by uneven harmonic oscillator functions. One can expand the eigenvalues $a_n(q_0)$ in a power series of q_0 and Eq. (29b) represents the first two terms of this expansion.[28]

Finally, Eq. (29c) has been obtained using the Wentzel-Kramers-Brillouin (WKB) quantization procedure. The phase $\frac{3}{4}$ results from the Bohr-Sommerfeld quantization condition, in which the left-hand turning point (infinite barrier) contributes the phase $\frac{1}{2}$, while the right-hand one (parabolic well) contributes the phase $\frac{1}{4}$.

Equations (27) and (19) can be used to express the electron energies by the eigenvalues of Eq. (14), as given approximately in Eqs. (29a)–(29c). After some simple algebraic manipulations we obtain

$$\varepsilon = \hbar k_x v_d + (1-\gamma^2)^{1/2} [(\varepsilon_g/2)^2 + \varepsilon_g D^{\pm}_{n,k_z}]^{1/2} - \frac{\varepsilon_g}{2} \, , \quad (30)$$

where

$$D^{\pm}_{n,k_z} = -a_n(q_0)(1-\gamma^2)^{1/2}\hbar\omega_c + \frac{\hbar^2 k_z^2}{2m_0^*} \pm \frac{1}{2} g_0^* \mu_B B \quad (31)$$

and $v_d = E/B$ is the drift velocity in crossed fields, transverse to both of them (for $\gamma < 1$).

With these equations, one can calculate the electron energies as a function of the subband index n, the normalized center coordinate q_0, the momentum $\hbar k_z$, and the spin orientation. However, for the purpose of optical considerations, it is more useful to know the energies as a function of the momentum $\hbar k_x$ rather than of the center coordinate q_0, since $\hbar k_x$ is conserved in direct optical transitions. Once the energy is obtained from Eq. (30) for a given q_0, one can calculate the corresponding k_x value from

$$k_x L = \frac{1}{\sqrt{2}} (1-\gamma^2)^{3/4} q_0 + k_d L \left[1 + 2\frac{\varepsilon}{\varepsilon_g} \right] . \quad (32)$$

This equation follows from Eqs. (16) and (17). Here k_d is defined as $\hbar k_d = m_0^* v_d$. Note that one can write

$$\gamma^2 = \left[\frac{2\hbar\omega_c}{\varepsilon_g} \right] (k_d L)^2 = \frac{2m_0 v_d^2}{\varepsilon_g} \, . \quad (33)$$

Using this procedure the dispersion of the hybrid subbands $\varepsilon_n(k_x)$ is obtained. Figure 2 shows the electron energies in the conduction band of InSb for a fixed electric and magnetic field versus $k_x L$ for $n=0,1,2$ and $k_z=0$. In the calculation, we used numerical values for the eigenvalues a_n of the parabolic cylinder functions.

As follows from the preceding discussion, large positive $k_x L$ values correspond to electrons in the bulk of the semiconductor, away from the barrier. The increase of the electron energies in this range is mainly due to the increase of the potential energy of the magnetic orbit center in the external electric field [see Eq. (38)]. The increase on the left-hand side is due to the fact that the electron is pressed very close to the barrier and oscillates rapidly in its vicinity (see Fig. 1). At large positive $k_x L$ values, the subbands for different indices n and spin orientations $\pm$ run parallel to each other, since the eigenvalues $a_n(q_0)$ become independent of q_0 ($-a_n \to n+\frac{1}{2}$). This allows one to observe sharp cyclotron resonance transitions. The magnetic field causes spin splitting of the subband energies that is highest for the electrons in the bulk ($q_0 \to \infty$). This features results from Eq. (31), in which the term

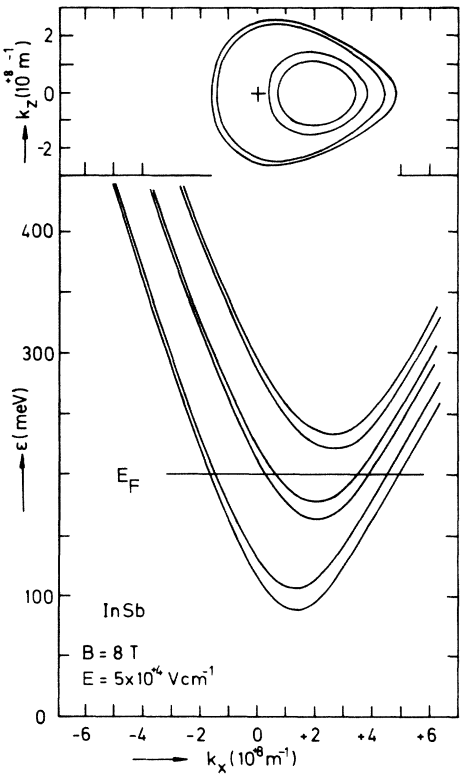

FIG. 2. Eigenenergies of inversion electrons in crossed fields calculated for InSb band parameters (magnetic case). In the upper part lines of constant Fermi energy E_F in (k_x, k_z) space are shown for the electron density $n_s = 1.5 \times 10^{12}$ cm^{-2}.

$\pm\frac{1}{2}g_0^*\mu_B B$ is independent of the center coordinate q_0, whereas the eigenvalue $a_n(q_0)$ strongly increases at center coordinates $q_0 \ll -1$, i.e., at large negative $k_x L$ values.

The cyclotron resonance energy $\varepsilon_2^+ - \varepsilon_1^+$ is visibly smaller than $\varepsilon_1^+ - \varepsilon_0^+$, which is a direct consequence of the nonparabolicity, well known from cyclotron resonance experiments on bulk InSb.[29]

In order to describe the occupancies of various subbands n, one has to calculate the lines of constant energy in (k_x, k_z) space. An example of such a calculation for the spin-split ground state $0^\pm$ and the first excited state $1^\pm$ is also shown in the inset of Fig. 2. Knowing the density of states:

$$\rho(k)dk_x dk_z = 1/(4\pi^2)dk_x dk_z$$

for each spin orientation, we can calculate the number of electrons contained within each Fermi line ($n_0^+ = 6.3\times10^{11}$ cm^{-2}, $n_0^- = 5.4\times10^{11}$ cm^{-2}, $n_1^+ = 2.0\times10^{11}$ cm^{-2}, $n_1^- = 1.3\times10^{11}$ cm^{-2}). The Fermi energy ε_F shown in Fig. 2 corresponds to the total surface density $n_s = 15\times10^{11}$ cm^{-2}.

Knowing the $k_x L$ values involved, one can calculate the range of corresponding center coordinates q_0. For the situation in Fig. 2, the electrons are contained between $-397 < y_0 < 293$ Å, so that the right-hand limit is, in fact, located in the bulk: $y_0 = 4.3R$. This means that the electrons with such orbit centers are in practice three-dimensional, i.e., their wave functions are no longer influenced by the barrier.

It follows from Fig. 2 that one should be able to excite electrons also near the surface, which will result in resonances at higher excitation energies. Such resonances have recently been observed.[30]

B. Magnetic case: Bulk limit

If the electrons are located sufficiently far away from the barrier, we may replace the boundary conditions [Eq. (22)] by the conditions $\phi(y = \pm\infty) = 0$. Such a problem has been considered before.[31] The eigenvalue problem of Eq. (26) then becomes identical to that of the harmonic oscillator (as long as $\omega^2 > 0$) and the quantization can be carried out immediately: $a_n = -(n + \frac{1}{2})$. The same result can be obtained from Eq. (29a), neglecting the exponential term. The explicit solutions for the electron energies are again given by Eq. (30), where D_{nk_z} no longer depends on q_0,

$$D_{n,k_z}(\gamma) = \hbar\omega_c(1-\gamma^2)^{1/2}(n+\tfrac{1}{2}) + \frac{\hbar^2 k_z^2}{2m_0^*} \pm \tfrac{1}{2}g_0^*\mu_B B \ . \tag{34}$$

To enable comparison with experiments, the cyclotron mass defined as

$$\hbar eB/m^* = \varepsilon_{n+1}^\pm - \varepsilon_n^\pm \tag{35}$$

is introduced. We carry out the calculation for $k_z = 0$, for which the combined density of states is the highest.

In Fig. 3 we plot cyclotron masses in InSb, calculated

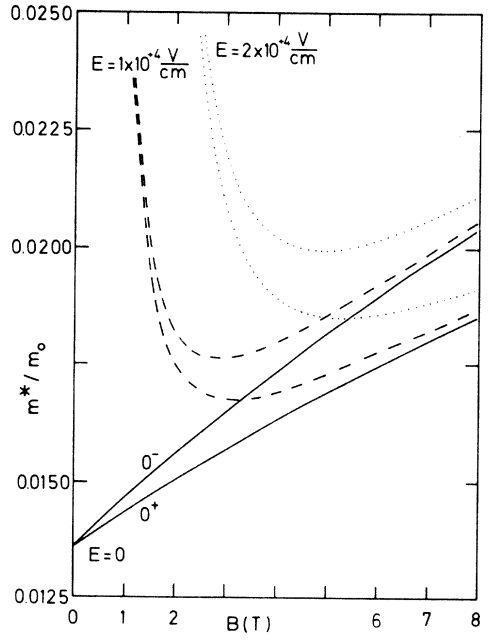

FIG. 3. Electron cyclotron masses in crossed fields calculated for InSb band parameters. The masses are given for the purely magnetic case ($E=0$) and for two constant electric fields (magnetic case, bulk limit).

with the use of Eqs. (30), (34), and (35) and the following parameters: $m_0^* = 0.0136m_0$, $\varepsilon_g = 0.250$ eV, and $g_0^* = -51.3$. The employed gap value is somewhat higher than the real one (0.236 eV), which is a consequence of the fact that in the theoretical model we have put the spin-orbit energy $\Delta = \infty$. The calculated masses for the spin-up transitions are in very good agreement with experiment,[32] confirming validity of our description. For comparison, we also show in Fig. 3 cyclotron masses ($0^\pm \to 1^\pm$) in the absence of an electric field. The corresponding curve for $E=0$ has been calculated from the expression

$$\varepsilon = [(\varepsilon_g/2)^2 + \varepsilon_g D_{nk_z}^\pm]^{1/2} - \frac{\varepsilon_g}{2} \tag{36}$$

where

$$D_{nk_z}^\pm = \hbar\omega_c(n+\tfrac{1}{2}) + \frac{\hbar^2 k_z^2}{2m_0^*} \pm \tfrac{1}{2}g_0^*\mu_B B \tag{37}$$

for $k_z = 0$. These formulas are obtained from Eqs. (30) and (34) for $E = \gamma = 0$. They have been widely used to describe magneto-optical and magnetotransport experiments in narrow-gap semiconductors.[33]

The results shown in Fig. 3 may be interpreted in the following way. At high magnetic fields $\gamma^2 \ll 1$, the electric term in the effective frequency ω is negligible: $\omega \simeq \omega_c$, and the increase of the cyclotron mass is due to the decrease of the cyclotron frequency with increasing electron energy as the magnetic field gets stronger. This is described by the square root in Eqs. (30) and (36) and goes back to the quadratic dependence of the eigenvalue $\lambda_\pm$ on the electron energy in Eq. (19).

At lower magnetic fields the electric term in ω becomes important [see Eq. (23)]. As the magnetic field B decreases it makes ω smaller and smaller ($\gamma^2 \rightarrow 1$) resulting in the strong enhancement of the cyclotron mass, as defined in Eq. (35). This is in sharp contrast to the $E=0$ case, in which only the first effect occurs, as is seen from Eq. (36) and the results in Fig. 3. The good agreement between experiment[32] and theory in both $E=0$ and $E\neq 0$ physical situations confirms the validity of our model for conduction electrons in InSb.

The one-band effective-mass approximation for electrons in crossed fields may be obtained from Eqs. (30) and (34) in the limit of large ε_g values. One can then approximate $(1-\gamma^2)^{1/2} \simeq 1-\gamma^2/2$. Developing the square root of the square brackets to terms linear in $D^{\pm}_{nk_z}$ and neglecting terms involving $1/\varepsilon_g$, one obtains finally

$$\varepsilon = \hbar\omega_c(n+\tfrac{1}{2}) + \frac{\hbar^2 k_z^2}{2m_0^*} \pm \tfrac{1}{2} g_0^* \mu_B B + eEk_x L^2 - \tfrac{1}{2} m_0^* \frac{E^2}{B^2} . \tag{38}$$

In this parabolic approximation, the transverse electric field shifts all Landau levels downwards by the same amount, so that its effect may not be observed in cyclotron resonance intraband experiments. However, as was first pointed out by Aronov,[5] the hole Landau levels are shifted upwards by the same transverse electric field and it is possible to observe a decrease of the interband energies in crossed fields using both absorptive and dispersive interband magneto-optical effects.[6]

C. Magnetic surface levels ($E=0$)

The above theory also applies to magnetic surface levels as studied on metals and semimetals.[34] In these materials the Fermi energy by far exceeds the cyclotron energy and magnetic surface levels become occupied also in the absence of an electric field ($E=0$). From Eq. (30) we obtain

$$\varepsilon_n(q_0) = \left[\left[\frac{\varepsilon_g}{2} \right]^2 + \varepsilon_g \left[-\hbar\omega_c a_i(q_0) + \frac{\hbar^2 k_z^2}{2m_0^*} \pm \tfrac{1}{2} g_0^* \mu_B B \right] \right]^{1/2} - \frac{\varepsilon_g}{2} , \tag{39}$$

where we have the simple relation $q_0 = \sqrt{2} k_x L$ between momentum and center coordinate [see Eq. (32)]. The result is illustrated in Fig. 4.

It can be seen that in the bulk limit (large k_x values) the energies do not depend on the electron position. Nonparabolic effects in the orbital and spin quantizations are clearly visible. The presence of barrier affects higher Landau levels more strongly, which is understandable since the higher states are more extended.

Nonparabolic effects in magnetic surface levels have previously been studied experimentally in bismuth and have been explained theoretically using the semiclassical one-band effective-mass approximation (EMA) and the subsequent introduction of a nonparabolic mass.[35] The present procedure gives a more complete account of nonparabolic magnetic surface levels starting from the two-band EMA including the electron spin.

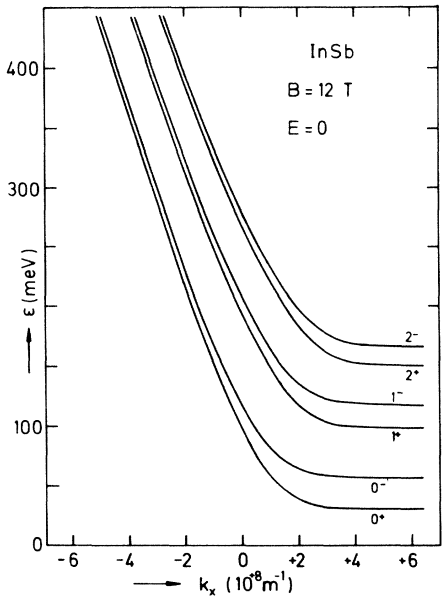

FIG. 4. Energies of magnetic surface levels calculated for InSb band parameters. The wave vector k_x can be related to the electron distance from the barrier, see text.

D. Electrons in crossed fields: Electric case

As the parameter γ of Eq. (24) approaches unity ($\omega \rightarrow 0$), the electron wave functions are progressively extended [$R \rightarrow \infty$, see Eq. (25)], and the existence of the barrier influences the motion more strongly. Also, the electrons whose initial positions are well within the bulk are now reflected from the barrier, so that their motion is basically electriclike, only weakly deflected by the magnetic field. In other words, the magnetic field is in this case not strong enough to prevent the electrons from reaching the interface. Finally, for $\gamma=1$, there is $\omega=0$ and $R=\infty$, so that without the barrier, the electron motion becomes unbound and the quantization disappears. Thus, in the unlimited space a sufficiently strong transverse electric field destroys the Landau quantization.[9] However, in the presence of an interface the electrons may not run away, since they are reflected from the barrier. For $\omega_c^2 < 2e^2E^2/\varepsilon_g m_0^*$ we have, in Eq. (14), a parabolic potential barrier instead of a parabolic potential well and the electrons oscillate between this barrier and the interface. The shape of the potential and the classical electron orbits are shown schematically in Fig. 5.

We consider first the case $\gamma=1$, i.e., the effective frequency $\omega=0$. For a given semiconductor with band-edge mass m_0^* and gap energy ε_g, this condition fixes the relative E and B field intensities: $B = E(2m_0^*/\varepsilon_g)^{1/2}$. Equation (14) has no quadratic term and its solutions are given by the Airy function. The energy quantization can be obtained using the boundary conditions in Eq. (22) and the known zeros of the Airy function.[27] However, a very good approximation to the eigenenergies (up to a fraction

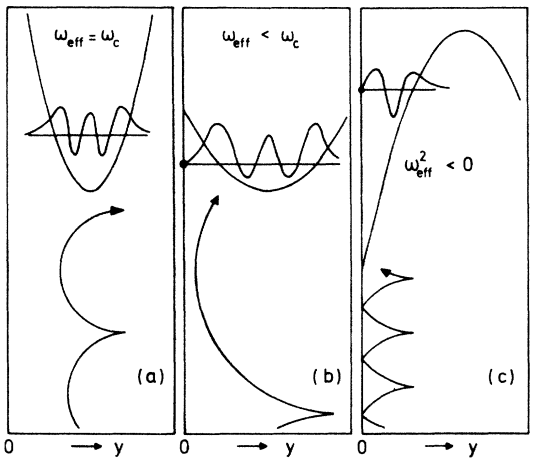

FIG. 5. Potential energies, wave functions, and classical orbits for magnetic (a,b) and electric (c) type of motion for inversion electrons in crossed fields.

of a percent[36]) can be obtained for this case with the use of the semiclassical WKB quantization procedure, which provides also a good insight into the physical situation.

We rewrite Eq. (14) in the form

$$\left[\frac{1}{2m_0^*}p_y^2+\alpha y\right]\phi=\lambda_\pm\phi\ , \tag{40}$$

where α and $\lambda_\pm$ are given in Eqs. (17) and (19), respectively, taking into account the fixed E/B ratio of the present case. We assume that $\alpha>0$, which means that the electrons are confined in a triangular potential well. In the WKB procedure, p_y is treated as a c number and it is determined from Eq. (40). The semiclassical quantization condition is

$$\int_0^{y_t} p_y\,dy=\hbar\pi(n+\tfrac{3}{4})\ , \tag{41}$$

where $y_t=\lambda_\pm/\alpha$ and the phase $\frac{3}{4}$ is the sum of the left-hand turning point contribution $\frac{1}{2}$ (infinite barrier) and the right-hand one $\frac{1}{4}$ (linear potential). After the integration we obtain a transcendental equation for the energies:

$$\frac{[x_\pm(1+x_\pm\beta)\pm\frac{1}{4}g_0^*(m_0^*/m_0)-\frac{1}{2}(k_xL)^2-\frac{1}{2}(k_zL)^2]^{3/2}}{1+2\beta x_\pm-k_xL\sqrt{2\beta}}$$
$$=\tfrac{3}{2}\pi(r+\tfrac{3}{4})\frac{1}{\sqrt{2\beta}}\ , \tag{42}$$

where, as before, $x_\pm=\varepsilon_\pm/\hbar\omega_c$ and $\beta=\hbar\omega_c/\varepsilon_g$. An example for the subband structure is given in Fig. 6 and will be discussed in the next section.

Now we consider the case $2e^2E^2/\varepsilon_g m_0^*>\omega_c^2$. Equation (26) is then the one for Weber parabolic cylinder functions of the second kind.[27] The energies may be quantized using the zeros of the Weber functions and the boundary condition (28). However, as in the case $\omega=0$, it is much simpler to use the semiclassical quantization procedure. For the case $B=0$, such a calculation has been done before.[21] We rewrite Eq. (14) in the form

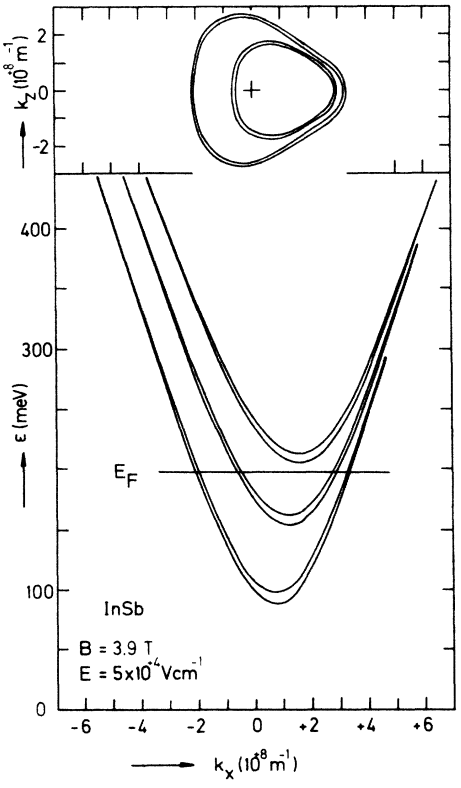

FIG. 6. Eigenenergies of inversion electrons in crossed fields calculated for InSb band parameters and the limiting case between magnetic and electric type of motion ($\omega=0$). In the upper part lines of constant Fermi energy E_F in (k_x,k_z) space are shown for the electron density $n_s=1.5\times10^{12}\ \mathrm{cm}^{-2}$.

$$\left[\frac{1}{2m_0^*}p_y^2+\alpha y-b^2y^2\right]\phi=\lambda_\pm\phi\ , \tag{43}$$

where α and $\lambda_\pm$ are defined in Eqs. (17) and (19), and

$$b^2=\frac{e^2(E')^2}{\varepsilon_g}\ . \tag{44}$$

E' has been defined as

$$E'=E(1-\delta^2)^{1/2}\ , \tag{45}$$

where

$$\delta^2=\left[\frac{\varepsilon_g}{2m_0^*}\right]\left[\frac{B}{E}\right]^2<1 \tag{46}$$

is an important parameter for the electric case. Treating p_y as a c number and completing the square in Eq. (43), we obtain

$$p_y=(2m_0^*)^{1/2}[\lambda_\pm-\alpha^2/4b^2+b^2(y-y_0)^2]^{1/2} \tag{47}$$

in which

$$y_0+\frac{\alpha}{4b^2}\ . \tag{48}$$

The Bohr-Sommerfeld integral takes the form

$$\int_0^{y_t}(-eE'y+eE'y_0-a_\pm)^{1/2}$$
$$\times(-eE'y+eE'y_0+a_\pm)^{1/2}dy=\hbar\pi(n+\tfrac{3}{4}), \quad (49)$$

where

$$a_\pm=\varepsilon_g^{1/2}\left[\frac{\alpha^2}{4b^2}-\lambda_\pm\right]^{1/2}. \quad (50)$$

The WKB phase in Eq. (49) is the same as in Eq. (41). The right-hand turning point y_t of the classical motion is determined by the zero of the first square root in Eq. (49). This gives $y_t=y_0-a_\pm/eE'$.

The integration in Eq. (49) can be carried out analytically and the result is

$$(A+B)A^{1/2}B^{1/2}+(B-A)^2\ln\left|\frac{B^{1/2}-A^{1/2}}{(B-A)^{1/2}}\right|$$
$$=\left[\frac{\varepsilon_g}{2m_0^*}\right]^{1/2}4eE'\hbar\pi(n+\tfrac{3}{4}), \quad (51)$$

where

$$A=eE'y_0-a_\pm,\quad B=eE'y_0+a_\pm. \quad (52)$$

Equation (51) represents a transcendental equation for the energies $\varepsilon_n(k_x,k_z)$ in the electric case ($\delta<1$). The energy is involved in y_0 [through α, see Eqs. (17) and (48)] and in $a_\pm$ [through $\lambda_\pm$ and α, see Eqs. (19) and (50)].

The general case of crossed fields may be reduced to the purely electric limit by putting $B=0$. This gives $\delta=0$ and $E'=E$, and after a simple manipulation A and B become

$$A=\varepsilon-\varepsilon_\perp,\quad B=\varepsilon_g+\varepsilon+\varepsilon_\perp \quad (53)$$

where

$$\varepsilon_\perp=\left[\left(\frac{\varepsilon_g}{2}\right)^2+\varepsilon_g\frac{\hbar^2}{2m_0^*}(k_x^2+k_z^2)\right]^{1/2}-\frac{\varepsilon_g}{2} \quad (54)$$

represents the energy of the free motion perpendicular to electric field. This is exactly the result obtained previously for the purely electric case.[21]

Figures 7(a) and 7(b) show electron energies $\varepsilon_n(k_x)$ for various subbands at $k_z=0$, calculated numerically from Eqs. (51)–(54) for the electric case ($\delta<1$). In Fig. 7(a), we illustrate the $B=0$ case, i.e., electric subbands. The curves are symmetric with respect to the $k_x=0$ value and the dependence $\varepsilon_n(k_x)$ is first quadratic and then becomes linear. Both features are seen directly from Eq. (54). Figure 7(b) shows subbands in a transverse magnetic field ($\delta^2=0.58$). The dispersion relations $\varepsilon_n(k_x)$ are asymmetric and the absolute values of the energies are shifted upwards (diamagnetic shift). This effect is somewhat obscured by the appearing spin splitting.

The energy minima shown in Fig. 7 can be directly observed in metal-to-semiconductor tunneling[37] or in magnetotransport experiments,[38] where discontinuities of the density of states are of importance. The shift of the energy minima to higher values with growing magnetic field agrees qualitatively with a perturbation treatment for a parabolic band.[17] On the other hand, in order to theoreti-

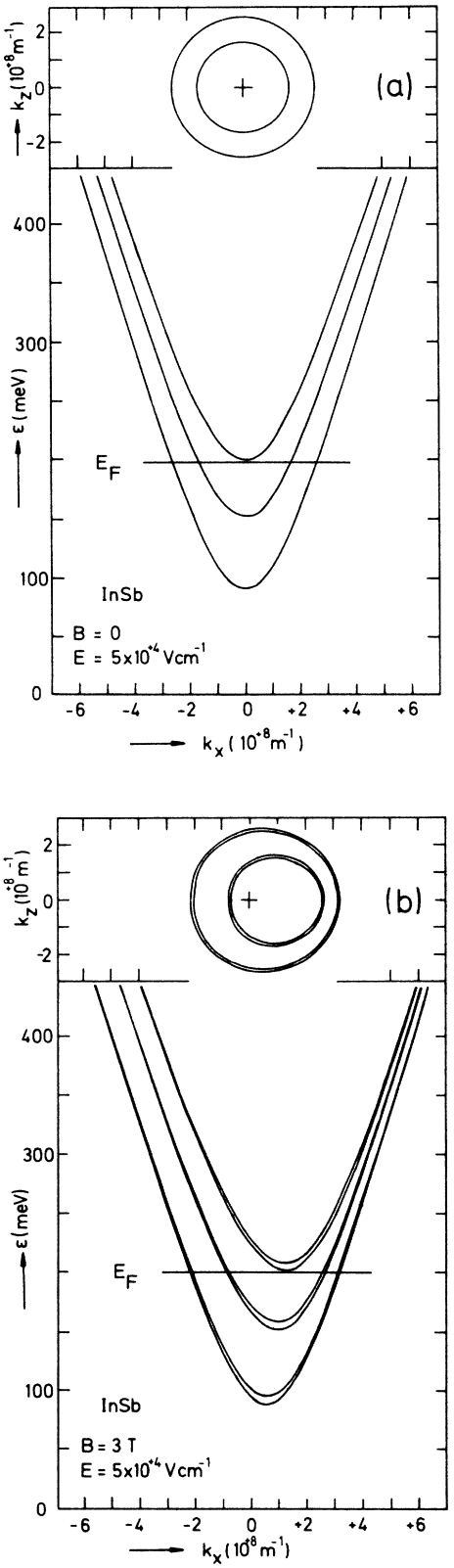

FIG. 7. Eigenenergies of inversion electrons (a) in an electric field (electric case, $B=0$) and (b) in crossed fields (electric case, $B\neq0$) calculated for InSb band parameters. In the upper part lines of constant Fermi energy E_F in (k_x,k_z) space are shown for the electron density $n_s=1.5\times10^{12}$ cm^{-2}.

cally investigate how a transverse magnetic field influences intersubband optical resonances, one has to first determine the value of k_x and k_z involved in the optical transitions for a given Fermi energy [see Figs. 7(a), and 7(b)].

Unlike in the magnetic case, the one-band EMA cannot be recovered from Eq. (51): The reason is that, as mentioned in the Introduction, the one-band EMA for any finite E/B ratio always gives a magnetic type of band structure [see Eq. (38)]. This will be discussed in greater detail in the next section.

In the purely electric case ($B=0$) we can recover the one-band EMA description. This is achieved by assuming that the energies, as counted from the bottom of the conduction band, are small compared to the gap value ε_g.

In this case one can develop the left-hand side of Eq. (51) into a power series of the variable

$$\eta=(\varepsilon-\varepsilon_\perp)/(\varepsilon_g+2\varepsilon_\perp)\ll 1 .$$

The first two terms of this expansion allows us to write Eq. (51) in the following approximate form:

$$\tfrac{8}{3}\eta^{3/2}+\tfrac{4}{5}\eta^{5/2}=4\pi(n+\tfrac{3}{4})\frac{1}{(\varepsilon_g+2\varepsilon_\perp)^2}\left[\frac{\varepsilon_g}{2m_0^*}\right]^{1/2}e\hbar E . \tag{55}$$

This formula can be used in case of weak nonparabolicity, e.g., for GaAs. Finally, when only the first term of the equation is retained and one assumes $\varepsilon_\perp \ll \varepsilon_g$, the well-known one-band EMA result for electric subbands in the triangular potential is obtained:

$$\varepsilon_n=\left[\frac{9\pi^2}{8m_0^*}\right]^{1/3}(n+\tfrac{3}{4})^{2/3}(e\hbar E)^{2/3}+\frac{\hbar^2(k_x^2+k_z^2)}{2m_0^*} . \tag{56}$$

IV. DISCUSSION: RELATIVISTIC ANALOGY

In Sec. III we have discussed a continuous transition of the electron motion from the magnetic to the electric type, as the E/B ratio increases. The corresponding eigenenergies are shown in our figures, beginning from the purely magnetic case and ending with the purely electric one. Our theory uses the coupled-band scheme, i.e., the multiband EMA, reduced for not too large energies to the two-band description, which takes into account the nonparabolicity and the spin properties of the conduction band in InSb-type materials. It should be emphasized again that for the unlimited space the one-band EMA always gives magnetic-type solutions, regardless of the E/B ratio. This is a consequence of the fact that the decoupling procedure leading to the one-band EMA for crossed fields is valid only when $(2m_0^*/\varepsilon_g)/(E/B)^2 \ll 1$, which can be regarded as the definition of the magnetic case.[7] On the other hand, the two-band EMA for the unlimited space gives magnetic-type and electric-type solutions, depending on the value of the E/B ratio. It should be noted, however, that the presence of an interface allows one to obtain electric-type solutions also within the framework of the one-band EMA. This is because the restriction of the motion by the interface makes it more electriclike, as is seen in Fig. 1. This feature is similar to the influence of scattering in magnetotransport, allowing an electric current to flow parallel to the electric field in the crossed-field configuration, which is an electric-type property.

In Fig. 8 we show the absolute electron subband energies taken at the minima of the dispersion curves $\varepsilon_n(k_x)$ at $k_z=0$ versus the magnetic field, starting from the values of purely electric subbands. It can be seen that not only the qualitative band structure goes continuously from one case to the other, as illustrated by the above figures, but also the calculated energies have this continuity, although they are calculated somewhat differently for the magnetic, intermediate, and electric case.

It was noticed some time ago that there exists a striking and far-reaching analogy between the behavior of electrons in narrow-gap semiconductors and relativistic electrons in vacuum.[3] The crossed-field configuration can serve as a spectacular illustration of this analogy.

In the absence of external fields, the energy-momentum relation resulting from the two-band model is given by the simplified Kane-formula

$$\varepsilon(\mathbf{p})=\left[\left[\frac{\varepsilon_g}{2}\right]^2+\varepsilon_g\frac{p^2}{2m_0^*}\right]^{1/2}-\frac{\varepsilon_g}{2} , \tag{57}$$

where $\mathbf{p}=\hbar\mathbf{k}$. It has the form of the relativistic dispersion relation for electrons in vacuum with the following correspondence: $\varepsilon_g \leftrightarrow 2m_0c^2$ and $m_0^* \leftrightarrow m_0$. It is easy to see that for the band described by Eq. (57), the electron velocity $v_i=\partial\varepsilon/\partial p_i$ may not exceed a maximum value of $u=(\varepsilon_g/2m_0^*)^{1/2}$. This property can be also deduced by analogy, observing that $c=(2m_0c^2/2m_0)^{1/2}$ and using

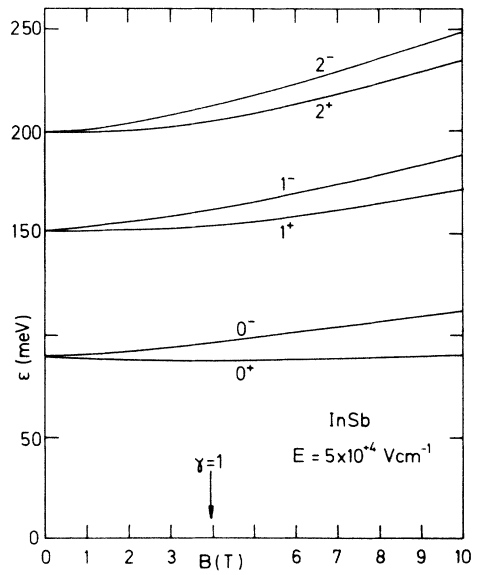

FIG. 8. Eigenenergies of inversion electrons in crossed fields versus magnetic field. The minima of the dispersion relations $\varepsilon(k_x)$ [cf. Figs. 2, 6, 7(a), and 7(b)] are calculated for InSb band parameters and a constant electric field $E=5\times10^{+4}$ V cm^{-1}. The magnetic field at which the transition from an electric to a magnetic type of motion occurs ($\gamma=1$) is indicated.

the above correspondence. The maximum velocity is almost the same for different materials, since to a good approximation there is $m_0^* \propto \varepsilon_g$ [cf. Eq. (20)]. u is of the order of 10^8 cm/s, i.e., considerably smaller than c.

In the presence of an external magnetic field, the expression for the electron energies in the bulk limit [Eq. (36)] has the form analogous to the expression for relativistic Dirac electrons.[39] Only the magnitude of the spin term is somewhat different, as the latter is determined in semiconductors by the spin-orbit interaction [see Eq. (21)], which is of the atomic origin and has no correspondence in the free-electron case.

It is well known that in the presence of crossed magnetic and electric fields, the electron drifts with a constant velocity v_d transverse to both fields. For free relativistic electrons, this velocity is $v_{dm}=E/B$ for $E/B<c$ (magnetic case) and $v_{de}=c^2B/E$ for $E/B>c$ (electric case) (see, e.g., Ref. 40). If a Lorentz transformation is made from the laboratory system to a system moving with the drift velocity, one eliminates from the equation of motion one of the two fields. In the magnetic case the electric field disappears and the magnetic field becomes $B'=B(1-v_{dm}^2/c^2)^{1/2}$. In the electric case, the magnetic field disappears and the electric field becomes $E'=E(1-v_{de}^2/c^2)^{1/2}$. Clearly, all other quantities of interest should be transformed as well to the moving system, in particular the four vector of momentum and energy.

According to the relativistic analogy, the conduction electron described by the two-band model moves in the presence of crossed fields with the drift velocity $v_{dm}=E/B$ for $E/B<u$ (magnetic case) and with $v_{de}=u^2B/E$ for $E/B>u$ (electric case). It can be directly verified that the Lorentz-type transformation (for $v_d \| x$ axis $p_y'=p_y$ and $p_z'=p_z$)

$$p_x'=\Gamma\left[p_x-\frac{v_d}{u^2}\varepsilon\right], \quad \varepsilon'=\Gamma(\varepsilon-v_d p_x) \tag{58}$$

where

$$\Gamma=\left[1-\frac{v_d^2}{u^2}\right]^{-1/2} \tag{59}$$

transforms Eq. (14) for crossed fields to either the purely magnetic or purely electric case, depending on whether the drift velocity v_{dm} or v_{de} is used. As far as the fields are concerned, this is seen immediately from Eqs. (23) and (45) for the two cases, respectively. Thus, in the magnetic case the characteristic parameter that was defined in Eq. (24) is simply $\gamma=v_{dm}/u$, and in the electric case [see Eq. (46)] we have $\delta=v_{de}/u$.

The result for electrons in the bulk of the semiconductor (magnetic case) given in Eqs. (30) and (34) may be interpreted in the following way: When a transformation to the moving system is made, only the magnetic field is left. The quantization can now be carried out with the result given in Eq. (36) in which $B'=B(1-\gamma^2)^{1/2}$ in the orbital part. Thus the energy in the moving system is given by the square root of the terms within square brackets in Eq. (30). However, the energy is observed in the laboratory system, so that a transformation back to this system is necessary according to Eq. (59) (with changed signs of v_d). This gives exactly the final result [Eqs. (30) and (34)], which is in agreement with the experimental data.[32] The energy difference measured in the cyclotron resonance experiment $\varepsilon_{n+1}-\varepsilon_n=\hbar\omega$ may be now interpreted as "the relativistic Doppler shift" $\omega=(1-v_{dm}^2/u^2)^{1/2}\omega_0$ where ω_0 is the frequency in the moving system (see, e.g., Ref. 40). This corresponds, in Eq. (30), to the factor $(1-\gamma)^{1/2}$ in front of the square root. In the special theory of relativity, the relativistic Doppler shift is regarded as a direct manifestation of the time dilatation.

A similar reasoning may be applied to the electric case. The results for crossed fields [Eqs. (51) and (52)] and those for the purely electric limit [Eqs. (53) and (54)] are related by the corresponding transformations of the fields and of the four vector of momentum-energy determined by v_{de}. The boundary condition at $y=0$ remains unchanged since v_{de} is parallel to the x direction.

V. SUMMARY

We have calculated eigenenergies of electrons near an interface in the presence of crossed electric and magnetic fields. The underlying geometric configuration is realized experimentally in metal-oxide-semiconductor structures or in semiconductor heterojunctions when a magnetic field is applied parallel to the interface. The theory is based on a three-level $\mathbf{k}\cdot\mathbf{p}$ model, which takes into account band's nonparabolicity and a strong spin-orbit interaction. The theory also provides a description of the limiting cases: electric subbands (for $B=0$) and magnetic surface states (for $E=0$).

The presented description may be applied to narrow-gap semiconductors with the conduction-band minimum at the Γ point, that is to InSb, InAs, $Ga_{1-x}In_xAs$, GaSb, and $Hg_{1-x}Cd_xTe$, but the general features apply also to other materials, for example to narrow-gap lead chalcogenides.

We have considered throughout uniform magnetic and electric fields, i.e., we have approximated the interface potential by a triangular potential well. This should be regarded as a rough approximation to a self-consistent potential, but it provides tractable analytical expressions for the hybrid states, which allow one an intuitive discussion of the physical situation.

The three-level effective-mass approximation describes two distinct types of solutions for electron states in crossed fields: the magnetic-type solution when the drift velocity $v_d=E/B$ is smaller than the maximum electron velocity $u=(\varepsilon_g/2m_0^*)^{1/2}$ possible in the conduction band, and the electric-type solution for higher E/B ratios.

We have emphasized a striking analogy of the described electron behavior in narrow-gap semiconductors to the behavior of relativistic electrons in vacuum. This analogy provides an interesting interpretation of the results and it can be advantageously used in the calculations.

ACKNOWLEDGMENTS

We thank Professor J. P. Kotthaus for his continuous encouragement, and the Deutsche Forschungsgemeinschaft for financial support.

*Permanent address: Institute of Physics, Polish Academy of Sciences, PL-02-668 Warsaw, Poland.

[1]W. Zawadzki, Surf. Sci. **37**, 218 (1973).
[2]K. von Klitzing, G. Dorda, and M. Pepper, Phys. Rev. Lett. **45**, 494 (1980).
[3]W. Zawadzki, in *Optical Properties of Solids,* edited by E. D. Haidemenakis (Gordon and Breach, New York, 1970), p. 179.
[4]J. C. Hensel and M. Peter, Phys. Rev. **114**, 411 (1959).
[5]A. G. Aronov, Fiz. Tverd. Tela (Leningrad) **5**, 552 (1963) [Sov. Phys.—Solid State **5**, 402 (1963)].
[6]Q. H. F. Vrehen and B. Lax, Phys. Rev. Lett. **12**, 471 (1964); Q. H. F. Vrehen, Phys. Rev. **145**, 675 (1966); W. Zawadzki, Q. H. F. Vrehen, and B. Lax, *ibid.* **148**, 849 (1966); Q. H. F. Vrehen, W. Zawadzki, and M. Reine, *ibid.* **158**, 702 (1967).
[7]J. Zak and W. Zawadazki, Phys. Rev. **145**, 536 (1966).
[8]H. C. Praddaude, Phys. Rev. **140**, A1292 (1965).
[9]W. Zawadzki and B. Lax, Phys. Rev. Lett. **16**, 1001 (1966).
[10]A. G. Aronov and G. E. Pikus, Zh. Eksp. Teor. Fiz. **51**, 281 (1966) [Sov. Phys.—JETP **24**, 188 (1967)]; *ibid.* **51**, 505 (1966) [**24**, 339 (1967)].
[11]W. Zawadzki, *Proceedings of the 9th International Conference on the Physics of Semiconductors* (Nauka, Leningrad, 1968), Vol. 1, p. 312.
[12]J. H. Crasemann, U. Merkt, and J. P. Kotthaus, Phys. Rev. B **28**, 2271 (1983).
[13]M. Horst, U. Merkt, and J. P. Kotthaus, Solid State Commun. **49**, 707 (1984).
[14]L. I. Magarill and A. V. Chaplik, Pis'ma Zh. Eksp. Teor. Fiz. **40**, 301 (1984) [JETP Lett. **40**, 1089 (1984)].
[15]R. E. Prange and T. W. Nee, Phys. Rev. **168**, 779 (1968).
[16]J. F. Koch and J. D. Jensen, Phys. Rev. **184**, 643 (1969).
[17]F. Stern and W. E. Howard, Phys. Rev. **163**, 816 (1967).
[18]W. Beinvogl, A. Kamgar, and J. F. Koch, Phys. Rev. B **14**, 4274 (1976).
[19]J. M. Luttinger and W. Kohn, Phys. Rev. **97**, 869 (1955).
[20]E. O. Kane, J. Phys. Chem. Solids **1**, 249 (1957).
[21]W. Zawadzki, J. Phys. C **16**, 229 (1983).
[22]M. H. Weiler, W. Zawadzki, and B. Lax, Phys. Rev. **163**, 733 (1967).
[23]H. Reisinger, Ph.D. dissertation, Technische Universität München 1983 (unpublished); W. Brenig and H. Kasai, Z. Phys. B **54**, 191 (1984).
[24]D. M. Larsen, J. Phys. Chem. Solids **29**, 271 (1968).
[25]R. Bowers and Y. Yafet, Phys. Rev. **115**, 1165 (1959).
[26]G. E. Marques and L. J. Sham, Surf. Sci. **113**, 131 (1982).
[27]J. C. P. Miller, in *Handbook of Mathematical Functions,* edited by M. Abramowitz and I. A. Stegun (Dover, New York, 1965), Chap. 19, pp. 685—720.
[28]P. Dean, Proc. Cambridge Philos. Soc. **62**, 277 (1966).
[29]E. D. Palik, G. S. Pikus, S. Teitler, and R. F. Wallis, Phys. Rev. **122**, 475 (1961).
[30]S. Oelting, U. Merkt, and J. P. Kotthaus, Surf. Sci. (to be published).
[31]W. Zawadzki and J. Kowalski, Phys. Rev. Lett. **27**, 1713 (1971).
[32]W. Zawadzki, S. Klahn, and U. Merkt, Phys. Rev. Lett. **55**, 983 (1985).
[33]W. Zawadzki, in *Physics of Narrow Gap Semiconductors,* Proceedings of the 3rd International Conference, edited by J. Rauluszkiewicz, M. Gorska, and E. Kaczmarek (Polish Scientific Publishers, Warszawa, 1978), p. 281.
[34]M. S. Khaikin, Adv. Phys. **18**, 1 (1969).
[35]M. Wanner, R. E. Doezema, and U. Strom, Phys. Rev. B **12**, 2883 (1975).
[36]F. Stern, Phys. Rev. B **5**, 4891 (1972).
[37]U. Kunze, J. Phys. C **17**, 5677 (1984); Phys. Rev. B **32**, 5328 (1985).
[38]W. Zhao, F. Koch, J. Ziegler, and H. Maier, Phys. Rev. B **31**, 2416 (1985).
[39]I. I. Rabi, Z. Phys. **49**, 507 (1928).
[40]J. D. Jackson, *Classical Electrodynamics,* 2nd ed. (Wiley, New York, 1975), pp. 522 and 582.